Benjamin Besser, Thomas Veltzke, Jochen A.H. Dreyer, Julia Bartels, Michael Baune, Stephen Kroll, Jorg Thöming, Kurosch Rezwan

A comparative experimental study on the deviation of the ideal selectivity in HDTMS-functionalized and untreated ceramic structures with pores in the upper mesoporous range

A comparative experimental study on the deviation of the ideal selectivity in HDTMS-functionalized and untreated ceramic structures with pores in the upper mesoporous range

Benjamin Besser [a], Thomas Veltzke [b], Jochen A.H. Dreyer [c], Julia Bartels [a], Michael Baune [b], Stephen Kroll [a, d, *], Jorg Thöming [b, d], Kurosch Rezwan [a, d]

[a] Advanced Ceramics, University of Bremen, Am Biologischen Garten 2, 28359 Bremen, Germany
[b] Center for Environmental Research and Sustainable Technology (UFT), University of Bremen, Leobener Strasse 1, 28359 Bremen, Germany
[c] School of Energy and Environment, City University of Hong Kong, 11 Science Park West Avenue, Shatin, Hong Kong Special Administrative Region
[d] Centre for Materials and Processes (MAPEX), University of Bremen, Am Fallturm 1, 28359 Bremen, Germany

ARTICLE INFO

Article history:
Received 17 February 2015
Received in revised form
20 May 2015
Accepted 25 June 2015
Available online 6 July 2015

Keywords:
Knudsen diffusion
Mesoporous ceramic membrane
Surface functionalization
Gas permeation
Carbon dioxide adsorption

ABSTRACT

Mesoporous ceramic capillary membranes with mean pore sizes of about 20 nm are prepared as model structures to investigate the influence of an altered surface chemistry on the flow behavior of gases. To modify the membrane surface, a wet chemical silanization process with hexadecyltrimethoxysilane (HDTMS) is used to gain an alkyl-functionalized surface. Structural and surface characterizations show that the surface chemistry is altered without affecting the mean pore diameter. For the non-functionalized membrane, single gas permeation measurements at 20 °C reveal ideal permselectivities which are in good agreement with the Knudsen theory. In contrast, the HDTMS-functionalized membrane shows permselectivities regarding carbon dioxide (CO_2) which deviate about 20% from Knudsen theory. The gas permeation measurements further indicate a relative flow enhancement for CO_2 in comparison to nitrogen (N_2), argon (Ar) and methane (CH_4). Adsorption and desorption isotherms of CO_2 and N_2 at 20 °C show a decreased specific adsorption capacity for both gases, while the adsorption selectivity for CO_2/N_2 is increased. This indicates a weaker interaction of gas molecules and membrane surface due to HDTMS functionalization. This weaker gas–solid interaction along with the increased adsorption selectivity is proposed as reason for the experimentally observed deviation of the permselectivities from Knudsen theory.

1. Introduction

In microfluidic systems, biotechnology and separation science, surface modifications of inorganic substrates are an active field of research. Especially in membrane science, this concept is applied to develop new and improved materials, for example to enhance the selectivity of porous, inorganic membranes for gas separation [1]. Mass transport in such mesoporous membranes is mainly governed by Knudsen diffusion, which results only in small separation factors. To increase the separation beyond Knudsen limit, the principle of surface-selective flow, which is attributed to selective adsorption and diffusion, can be utilized. Surface modifications are applied to increase the concentration of a specific adsorbable gas species on the surface to favor surface diffusion [2].

Processes using silane precursors provide a versatile tool to functionalize and tailor the membrane surface [3]. The surface functionality can be adjusted easily due to a broad spectrum of available silane molecules with different functional groups for example amino-, carboxyl- or alkyl-groups and spacer length, often ranging from C_3–C_{18} [4–6]. In particular, when focusing on CO_2 adsorption, amine-functionalizations show a high potential and are therefore subject in recent investigations [7,8]. For example, Stoltenberg and Seidel-Morgenstern [2], along with Ostwal et al. [9] and Sakamoto et al. [1] used an amine-modification to increase the CO_2/N_2 selectivity of mesoporous silica membranes. Furthermore, the effect of a membrane

* Corresponding author. Advanced Ceramics, University of Bremen, Am Biologischen Garten 2, 28359 Bremen, Germany. Tel.: +49 421 218 64933; fax: +49 421 218 64932.
E-mail address: stephen.kroll@uni-bremen.de (S. Kroll).

http://dx.doi.org/10.1016/j.micromeso.2015.06.042

functionalization with organosilanes showing different alkyl-chain lengths on the selectivity of especially heavier hydrocarbons [3,10,11] or for purification of aggressive gases such as chlorine [12] has been investigated.

According to Koros and Mahajan [13], the key requirements for membranes are durability, productivity and separation efficiency. The aimed performance optimum for membranes is therefore a high flux combined with a high selectivity. In general, a bigger pore size and a higher porosity results in a higher flux (permeability). Nevertheless, the contribution of surface diffusion is decreasing with increasing pore sizes, thus limiting an optimization. Therefore, the used membranes in the aforementioned studies possess pore sizes in the lower mesoporous region around 2–10 nm, since high separation factors are aimed. According to the general opinion in the literature, surface diffusion is supposed to be negligible in pores in the upper mesoporous range (10–50 nm) as well as macropores (>50 nm) [12,14,15]. In fact, solely Knudsen diffusion is considered as the main governing transport mechanism in the upper mesoporous region >10 nm [16].

In the Supporting Material of asymmetric inorganic membranes gas transport usually occurs in pores >10 nm. Until now, adsorption effects such as surface diffusion are neglected in such pores. In this study, deviations from the general rule stated above are observed by investigating the gas diffusion in inorganic membranes with pore sizes in the upper mesoporous region (>10 nm). Here, yttria stabilized zirconia (YSZ) as ceramic material and a well-established extrusion process are used to fabricate capillary membranes serving as model structures for gas permeation measurements. To affect the gas transport, a wet-chemical silanization process is used to immobilize an alkyl silane (hexadecyltrimethoxysilane, HDTMS) onto the surface showing a C_{16}-chain as functional group. Both, the non- and HDTMS-functionalized membranes are characterized by microstructural analysis with focus on pore size, porosity and specific surface area to ensure comparability. Single gas permeation measurements are conducted with argon (Ar) and nitrogen (N_2) as representatives for inert gases, as well as carbon dioxide (CO_2) and methane (CH_4) as gases with a more complex molecule structure and a higher interaction potential. Furthermore, adsorption/desorption measurements using N_2 and CO_2 are performed at 20 °C.

2. Experimental

In this section the used materials are briefly presented, followed by an introduction into the processing and functionalization route. Afterwards, the used material characterization methods are described, including structural analysis, characterization of the surface functionalization, as well as gas permeation and adsorption measurements.

2.1. Materials

The zirconia powder and reagents were purchased from commercial sources and used without further purification. The yttria (3 mol%) stabilized zirconia powder (YSZ, VP Zirkonoxid 3-YSZ, Lot. 3157061469) was obtained from Evonik Industries, Germany. Furthermore, for slurry preparation, 3-aminopropyltriethoxysilane (APTES, 99%, product number 440140, Lot. SHBC8357V) as dispersant and polyvinyl alcohol (PVA, fully hydrolysed, product number P1763, Lot. SLBC9027V) as binder were obtained from Sigma–Aldrich Chemie GmbH, Germany. Sulfuric acid (H_2SO_4, 95–97%, product number 30743, Lot SZBD2030V) as well as hydrogen peroxide ((H_2O_2, ≥35%, product number 95299, Lot SZBD2410V) for membrane surface hydroxylation were provided from Sigma–Aldrich Chemie GmbH, Germany. For membrane surface modification acetone (≥99%, product number 00585, Lot. SZBB0100V) used as organic solvent was purchased from VWR International, Belgium, and hexadecyltrimethoxysilane (HDTMS, 90%, product number AB111166, Lot. 1010563) was provided by ABCR, Germany. Double deionized water with an electrical resistance of 18 MΩ (Synergy®, Millipore, Germany) was used for all experiments.

2.2. Capillary membrane preparation

To prepare YSZ capillary membranes an extrusion process is used as described by Werner et al. [17]. A schematic overview of the processing route for membrane fabrication is given in Fig. 1A. Four ingredients are used for slurry preparation, namely YSZ-nanopowder (79 wt.%, primary particle size 30 nm), double deionized water as solvent (21 wt.%), APTES as dispersant (5 dwb.%) and PVA as binder (6 dwb.%). Here, dwb refers to "dry weight basis" of the YSZ nanopowder. Accordingly, all additives are specified based on the powder content in relation to $\text{dwb.\%} \equiv m_{\text{additive}}/m_{\text{powder}} \cdot 100$. In contrast to Werner et al. [17], first, PVA is slowly dissolved in hot water (≈80 °C). Afterwards, YSZ powder, PVA-solution and APTES are mixed in a planetary ball mill (PM400 from Retsch, Germany) for 3 h at 350 rpm changing the rotation direction every 5 min. The obtained homogeneous slurry is then shaped into capillaries using a self-made lab extruder, equipped with an extrusion die of 2 mm diameter and a pin of 1 mm [18,19]. The resulting green bodies are dried at room temperature (RT) for at least two days, followed by final sintering for 2 h at 1050 °C (the detailed sintering program is given in [19]).

2.3. Membrane surface functionalization

The membrane surface modification is performed by a two-step, wet-chemical process consisting of surface activation by hydroxylation followed by surface functionalization via silanization as schematically shown in Fig. 1B. A silane molecule is supposed to condensate and bind covalently onto an existent surface hydroxyl group using a water molecule as reaction partner [4]. To increase the amount of available hydroxyl groups and therefore increase the amount of bonding sites on the membrane surface, the membranes are primarily treated with freshly prepared Piranha solution (95–97% H_2SO_4:35% H_2O_2, 3:1, v/v) for 30 min as suggested by Kroll et al. [20]. Afterwards, the membranes are washed with double deionized water until neutral pH is reached, subsequently followed by drying at 70 °C for 24 h.

Secondly, the activated membranes are functionalized with HDTMS according to previous works [21]. The modification is carried out using a 0.2 M HDTMS solution where a acetone-water mixture (95:5, v/v) served as solvent. The membranes are incubated for 16 h at 80 °C under reflux. After incubation, the membranes are washed three times with acetone followed by drying for 2 h at 70 °C.

2.4. Membrane characterization

2.4.1. Membrane structure

To ensure the comparability between the untreated and the HDTMS-functionalized material, detailed structural analyses are carried out. Therefore, the membranes are characterized in terms of pore size distribution, mean pore size (d_{50}), relative pore volume, open porosity and specific surface area. The pore size distribution and the resulting mean pore diameter, along with the

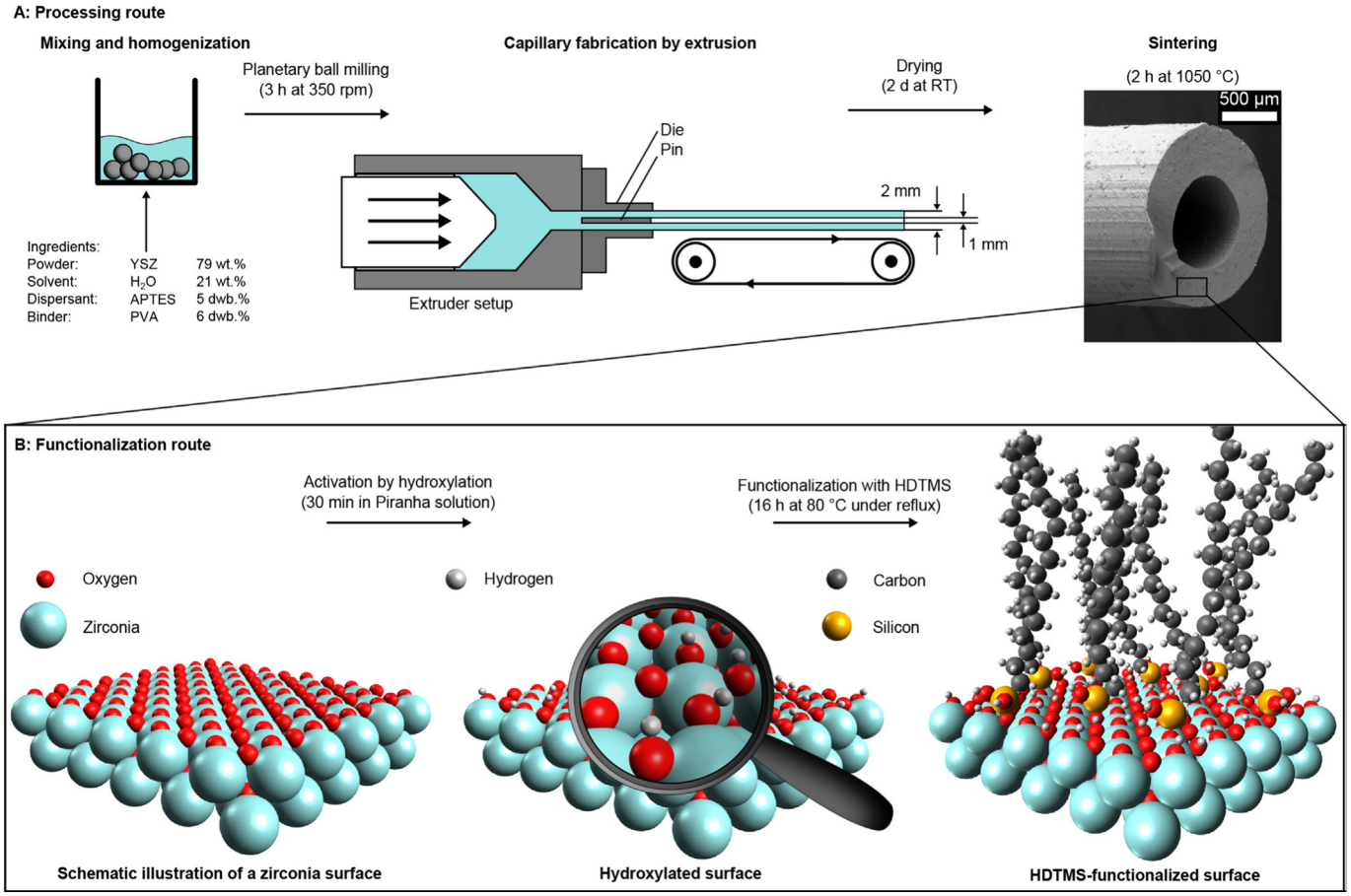

Fig. 1. Schematic overview of the slurry preparation, extrusion and sintering process (A), as well as the illustrated membrane functionalization process (B) through activation by hydroxylation and subsequent silanization using hexadecyltrimethoxysilane (HDTMS).

relative volume and the open porosity are determined by mercury intrusion porosimetry using a Mercury Porosimeter Pascal 140 and 440 (POROTEC GmbH, Germany). The specific surface area is measured by nitrogen adsorption at −196 °C according to BET method using a BELSORP-mini II (Bel Japan Inc., Japan). Prior to the gas adsorption measurements the membrane samples are degassed for at least 3 h at 120 °C and reduced pressure (≤ 2 mbar) followed by cooling to RT under argon atmosphere (≥30 min). Furthermore, the membrane microstructures are visualized by scanning electron microscopy (SEM) using a field-emission SEM SUPRA® 40 (Zeiss, Germany).

2.4.2. Membrane surface functionalization

The surface functionalization is characterized by thermogravimetry (TGA) and carbon content measurements. Thermogravimetry and differential scanning calorimetry (DSC) experiments are performed with a TGA/DSC1 Star System (Mettler Toledo, Germany). About 70 mg of the membrane samples are placed in an alumina crucible and heated from 30 to 900 °C (heating rate 10 °C/min) while flushing the sample with O_2 (30 mL/min). The amount of total carbon (TC) and inorganic carbon (IC) is measured using an SSM-500A solid sample module (Shimadzu, Japan). For TC measurements, about 50 mg membrane material is placed in a crucible and heated to 900 °C operating in oxygen (O_2) atmosphere. The IC is determined by placing about 100 mg membrane material in a crucible, adding sulfuric acid, and heating the sample to 200 °C. The amount of CO_2 formed during TC and IC experiments, respectively, is determined by an infrared (IR) detector (TOC-V, Shimadzu, Japan) and normalized to the exact sample weight.

2.4.3. Single gas permeation measurements

Single gas dead-end permeation measurements are performed with four different gases, namely argon (Ar), nitrogen (N_2), carbon dioxide (CO_2) and methane (CH_4), as schematically shown in Fig. 2A. A detailed description of the used measurement system is given by Veltzke et al. [22,23]. The samples are prepared by integrating the membrane capillaries into an alloy-sample holder using a two-component epoxy resin adhesive (UHU Plus endfest 300, UHU GmbH & Co. KG, Germany) as shown in Fig. 2B. For each membrane type, three different samples from separate processing batches, including all processing steps as depicted in Fig. 1 and indicated in Fig. 2C are used. Prior to the gas permeation measurements the membranes are heated to 120 °C for 3 h to desorb moisture. To ensure purity of the applied gas for the measurement, the whole system is evacuated and purged three times with the ongoing test gas. Afterwards, the membrane is flushed with the test gas for 60 s. All measurements are performed at 20 °C and 800 mbar dead-end pressure. As indicted in Fig. 2A, temperature and pressure on both sides, as well as the molar flow rate are measured and the data is logged at a frequency of 6 Hz. For each measurement the flow is measured at nine different pressure drops. After adjusting a certain pressure difference and waiting until the system has reached a steady-state condition, the data is averaged over 120 s.

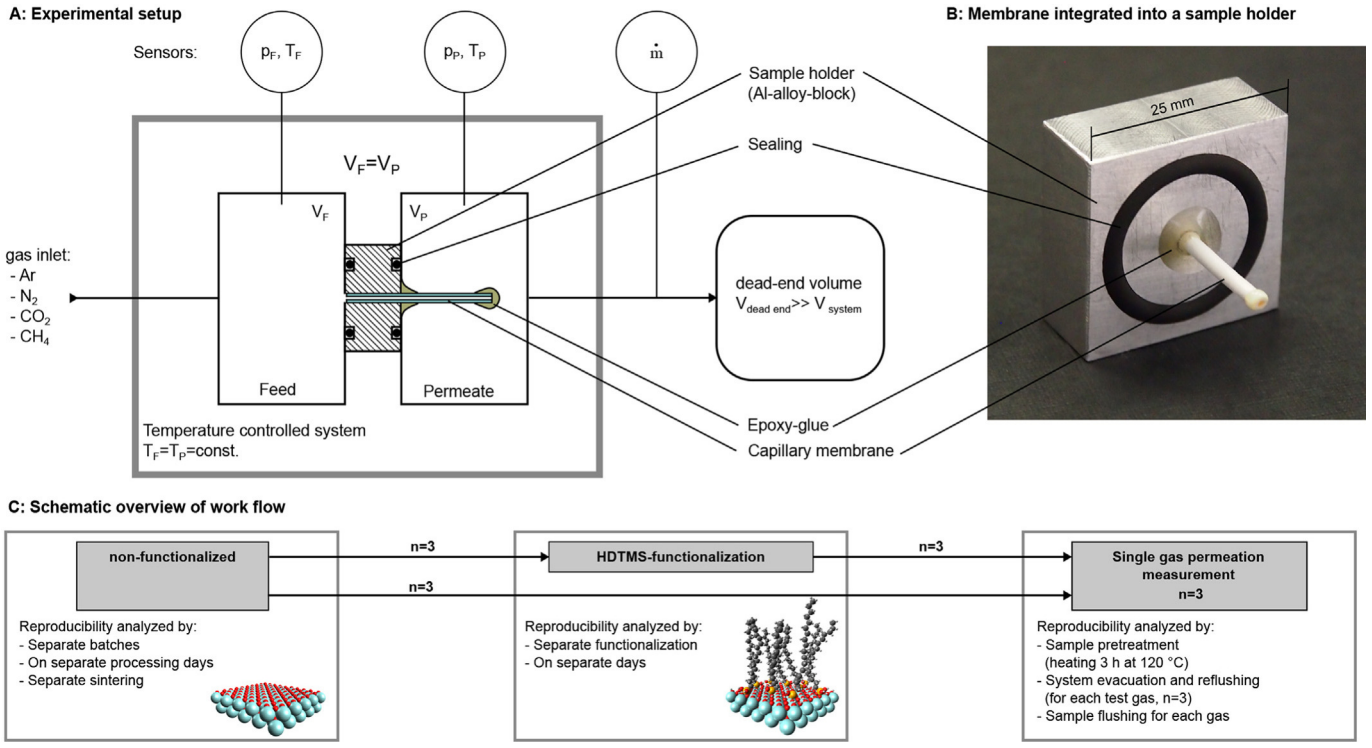

Fig. 2. Schematic overview of the experimental setup for single gas permeation measurements operating in dead-end mode (A). Mass flow, temperature and pressure are measured on both sides (feed and permeate) while the pressure difference between feed and permeate ($p_P - p_F$) is controlled. The overall system temperature is controlled and constantly kept at 20 °C. Notation for indices: F: Feed, P: Permeate. Photograph of a capillary membrane integrated into a sample holder (B). Schematic overview of the work flow (C).

In total, each measurement is performed three times to ensure reproducibility. The relation between the pressure difference and the molar flow is used for data evaluation. Particularly, after linear regression of the molar flow onto the pressure difference, the ratio of the slopes from two different gases is used to calculate the ideal permselectivity, as:

$$\alpha_{i,j} = \frac{(\partial \dot{n}/\partial p)_i}{(\partial \dot{n}/\partial p)_j}, \tag{1}$$

with $\dot{n}$ as the molar flow rate of gas i or j.

2.4.4. Evaluation of gas permeation measurements

In order to compare the non-functionalized and the HDTMS-functionalized membranes the Knudsen theory is used, which represents the dilute gas flow in mesoporous structures. According to Knudsen [24], molecular diffusion in porous solids is driven by diffuse reflection of the molecules from the pore walls, predominating when the pore diameter (d) is smaller than the mean free path of the gas molecules (λ). The rarefaction of a gas is quantified by the Knudsen number. Based on the kinetic theory of gases assuming a Maxwell–Boltzmann distribution, the Knudsen number can be defined as:

$$Kn = \frac{\lambda}{d} = \frac{k_B T}{\sqrt{2}\pi\sigma^2 p d}, \tag{2}$$

where k_B is the Boltzmann constant, T is the temperature, σ is the collision diameter of the gas molecule and p is the pressure. Furthermore, d is a representative physical length scale, in this case the mean pore diameter of the membrane (d_{50}). According to the Knudsen theory it can be shown that the molar flow of a gas is inversely proportional to the square root of its molar mass, assuming constant temperature and pressure. Therefore, Knudsenselectivities can be calculated for specific gas pairs, knowing their molar mass M, according to:

$$\alpha_{Kn,ij} = \sqrt{\frac{M_j}{M_i}}. \tag{3}$$

In the following, the molar mass of the heavier gas is defined as numerator (M_j), resulting in Knudsenselectivities always >1. According to this definition and the definition of indexes in Equation (1) in Section 2.4.3, the slope of the heavier gas is therefore defined as the denominator ($(\partial \dot{n}/\partial p)_j$) for the calculation of the permselectivity. To compare the non-functionalized and HDTMS-functionalized membranes, the permselectivity and the Knudsenselectivity are used as key values.

2.4.5. Gas adsorption and desorption measurements

To investigate the interaction between gas and surface under conditions similar to the gas permeation measurements (see Section 2.4.3), adsorption/desorption isotherms of N_2 and CO_2 are performed at 20 °C using a Belsorp-Max (Bel Japan Inc., Japan). Additionally, to identify the existent specific surface area, nitrogen adsorption at −196 °C according to BET method are performed with the same measurement device. To analyze the adsorption capacities, the adsorption/desorption isotherms at 20 °C are normalized to the measured specific surface area and recalculated to μmol/m^2. For the above mentioned experiments, about 350 mg membrane material is used and pretreated by degassing for at least 3 h at 120 °C and reduced pressure ($\leq$ 2 mbar), followed by cooling to RT under argon atmosphere ($\geq$ 30 min).

3. Results and discussion

3.1. Membrane structure

As given in Equation (2), the Knudsen number describes the relation between the condition of the gas and the porous structure. Accordingly, the governing transport mechanism is highly dependent on the porous structure represented by the mean pore diameter of the membrane. For this reason, a detailed structural analysis is essential to ensure comparability of the non-functionalized and HDTMS-functionalized membrane structures. In Fig. 3, a non-functionalized (part A) and an HDTMS-functionalized (part B) membrane are compared, showing quantitative pore size distributions and open porosities derived from mercury intrusion porosimetry as well as SEM micrographs for qualitatively analysis (insets). Both, the non-functionalized and the HDTMS-functionalized membrane show similar monomodal and narrow pore size distributions in the mesoporous range with a sharp increase in the relative pore volume below 30 nm. This indicates that the basic, overall pore structure of the membrane is not influenced by the applied surface functionalization using HDTMS, which can also be confirmed by the corresponding SEM micrographs of the membrane surfaces as shown in the insets in part A and B of Fig. 3. Due to the applied moderate sintering temperature of 1050 °C for 2 h, a relatively high open porosity of the non-functionalized membrane of around 44% is achieved. By functionalization using HDTMS a significant decrease of about one-fourth in open porosity is obtained, as shown in part B of Fig. 3. For this particular measurement, a small content of open porosity (3%) is already detected at bigger pore diameters > 0.1 μm, which is attributed to measurement artifacts, since no pores are detected in this region for the untreated membrane material (see Fig. 3A). Nevertheless, the characteristic shape of the pore size distribution with a sharp increase in the relative pore volume below 30 nm remains after functionalization.

Table 1 summarizes the results derived from mercury porosimetry and BET measurements of non- and HDTMS-functionalized membranes from individual processing batches (n = 3) and surface functionalizations (n = 3). For specifying the pore size range based on the distribution of relative pore volume, a threshold of 2% is set to exclude artifacts. The pore size ranges of both membrane types are similar, but slightly shifted to smaller pore sizes after functionalization with HDTMS. This results in a smaller mean pore diameter (d_{50}) of 18.1 nm for the HDTMS-functionalized membrane compared to the non-functionalized membrane (22.2 nm). Based on the molecule length of HDTMS of around 2 nm a decrease of the mean pore diameter of around 4 nm is plausible due to the surface functionalization. In agreement with the open porosity results (Fig. 3), the specific surface area of the membrane is decreased by 39% due to applied HDTMS functionalization. This behavior is also described by Kuraoka et al. [11] for surface functionalizations using organosilanes with long alkyl chains, where a decrease of about 96% in specific surface area is attributed to a C_{18}-chain functionalization of porous glass membranes with pore sizes of about 4 nm. As a reason for the decrease in specific surface area, pore filling and blocking by immobilization of the long chain molecules is identified by Kuraoka et al. Accordingly, this is also assumed being a reason for the reduction of the porosity and specific surface area due to HDTMS functionalization in this study. Introducing a certain amount of molecules into a limited pore volume inevitable causes a reduction of volume which is represented by the decrease in porosity.

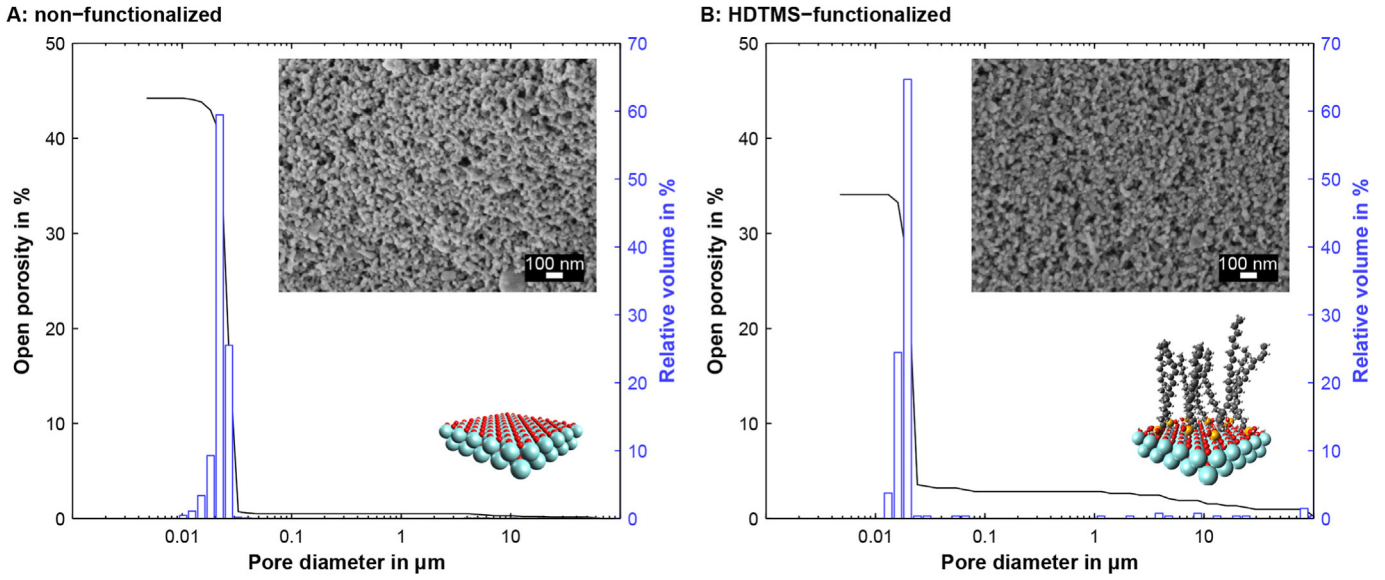

Fig. 3. Pore size distributions and open porosities of the non-functionalized (A) and the HDTMS-functionalized membrane (B) obtained from mercury intrusion porosimetry along with SEM micrographs of the corresponding membrane surfaces (inset). The membranes feature a very narrow pore size distribution which is not influenced by the surface functionalization.

Table 1
Structural properties of the non-functionalized and HDTMS-functionalized membranes measured by mercury porosimetry and nitrogen adsorption. While the open porosity and the specific surface area are decreased after HDTMS-functionalization, the mean pore diameter is not significantly influenced by the surface functionalization.

Membrane	Pore size range in nm	Mean pore diameter d_{50} in nm	Open porosity in %	Specific surface area in m^2/g
Non-f.	17.0 ± 0.5–29.1 ± 3.2	22.2 ± 1.4	43.7 ± 0.6	20.1 ± 0.5
HDTMS-f.	14.2 ± 0.3–21.3 ± 0.5	18.1 ± 2.0	32.3 ± 2.0	12.3 ± 0.9

Furthermore, small pores and narrow interconnections may be blocked due to steric hindrance of the long HDTMS molecules, resulting in a decrease of specific surface area. The Knudsen number and the ideal selectivity (see Equations (2) And (3)) are not influenced by the open porosity or specific surface area. Therefore, the governing transport mechanism for gases is independent of these two membrane properties. In contrast, the mean pore diameter directly influences the Knudsen relation and plays an important role for the analysis of gas transport mechanisms in porous structures. The results show that the mean membrane pore diameter is decreased only slightly due to HDTMS-functionalization and therefore the governing transport mechanisms within both membrane types are considered comparable.

3.2. Surface functionalization

The decrease in porosity and specific surface area indicates a successful HDTMS functionalization and the presence of HDTMS molecules on the membrane surface. For further characterization of the membrane functionalization and for quantification of the silane-molecules attached to the surface, additional analysis are performed including TGA, as well as total- and inorganic carbon content measurements. Fig. 4A shows an exemplary TGA/DSC measurement of a non-functionalized and an HDTMS-functionalized membrane from the same processing batch. The non-functionalized membrane only shows little weight loss, mainly below 200 °C, which is related to water desorption. After HDTMS functionalization, the TGA signal shows a significant increase in weight loss above 200 °C, in particular 3.72 wt.% between 200 °C and 600 °C. Likewise, the associated DSC measurement shows a high heat-uptake above 200 °C. In contrast, the DSC signal obtained from the non-functionalized membrane shows no heat-uptake. In summary, considering the TGA and DSC results for both membrane types, a degradation of the HDTMS molecule above 200 °C is suggested. For additional analysis of the weight loss, carbon content measurements are performed to further detect the degradation of the C_{16}-chains from the HDTMS molecules. Fig. 4B compares the results of the TGA and TC measurements. Using the non-functionalized membrane as reference, the specific weight loss due to HDTMS degradation determined by TGA is $m_{TGA} = 3.62 \pm 0.19$ wt.%. In contrast, the amount of carbon (TC) measured by the IR detector can be quantified to 3.13 ± 0.22 wt.%. Since the TC measurement only detects carbon, the hydrogen atoms from the desorbing HDTMS molecules (C_{16} H_{33}) are not considered by this technique. Therefore, to estimate the total mass loss due to HDTMS desorption, the TC result ($m_{C,TC}$) is recalculated with respect to the C/H relation ($n_C = 16$ and $n_H = 33$) according to $m_{HDTMS,TC} = m_{C,TC} \cdot (n_C \cdot m_C + n_H \cdot m_H)/(n_C \cdot m_C)$ using $m_C = 12.011$ and $m_H = 1.008$ as atomic weights. The resulting calculated total mass loss of $m_{HDTMS,TC} = 3.67 \pm 0.26$ wt.% based on the TC detection is in good agreement with the measured weight loss by TGA measurements ($m_{TGA} = 3.62 \pm 0.19$ wt.%).

In addition to the TC detection, inorganic carbon content measurements are performed to ensure an organic origin of the detected total carbon. Table 2 summarizes the results of the carbon content and weight loss measurements for the non- and HDTMS-functionalized membranes based on three processing batches and HDTMS-functionalizations. For all IC measurements, the signal is below detection limit (<0.01 wt.%), confirming that the measured TC content is organic carbon. In

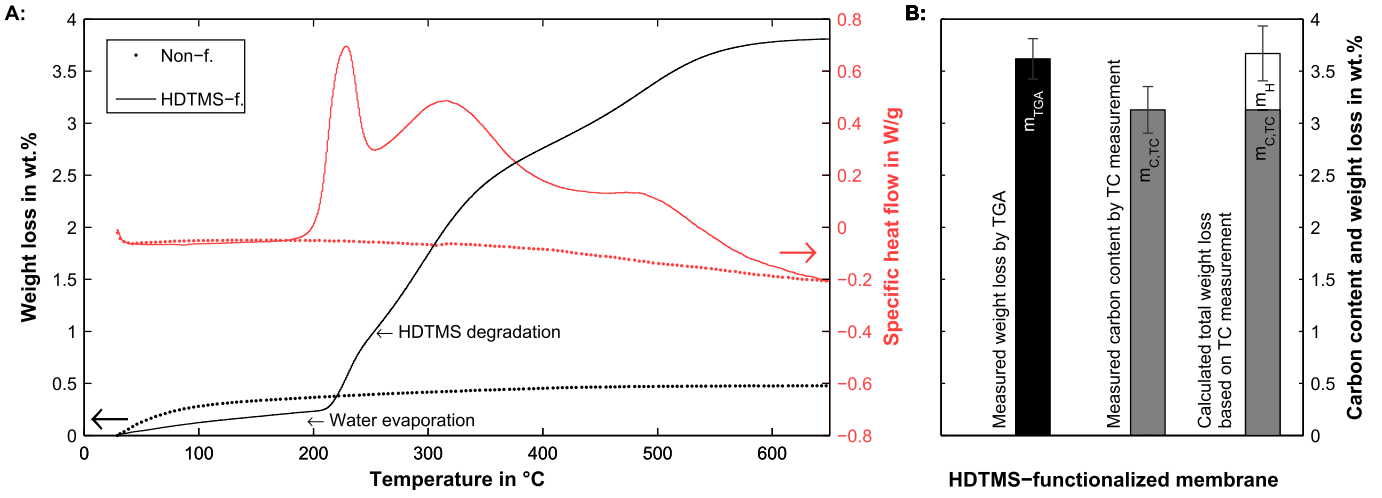

Fig. 4. Comparison of the estimated weight loss (resulting from total carbon (TC) content measurements) with the weight loss determined by TGA measurement (A), as well as two exemplary TGA/DSC measurements of a non-functionalized and an HDTMS-functionalized membrane (B). The results from both measurement techniques are in good agreement.

Table 2
Carbon content of the non-functionalized and HDTMS-functionalized membranes derived from total carbon and inorganic carbon measurements as well as the calculated (based on TC measurements) and the measured weight loss from TGA along with the calculated functional groups per membrane surface area.

Membrane	Carbon content in wt.%		Weight loss in wt.%		Functional groups[a] in	
	Total	Inorganic	Calculated[b]	Measured[c]	μmol/m²	Groups/nm²
Non-f.	<0.01	<0.01	0	0.11 ± 0.05	0	0
HDTMS-f.	3.13 ± 0.22	<0.01	3.67 ± 0.26	3.73 ± 0.19	5.20 ± 0.07	3.13 ± 0.04

[a] Calculated amount of functional groups using specific surface area and measured weight loss from TGA.
[b] Calculated weight loss due to degradation of HDTMS (C_{16} H_{33}) based on the measured total carbon content.
[c] Measured weight loss by TGA measurement (weight loss between 200 and 600 °C).

general, the results from both types of measurements are highly reproducible and show similar results, suggesting that both techniques are suitable for quantification of HDTMS molecule contents. Table 2 also presents the calculated amount of functional groups in μmol/m^2 and groups/nm^2. Here, the TGA measurement results are normalized to the specific surface area of the non-functionalized membranes (a) and recalculated according to $c_{HDTMS} = m_{TGA} \cdot M_{HDMTS}/a$ using the molar mass of HDTMS ($M_{HDTMS} = 346.63$ g/mol). Accordingly, the calculated amount of functional HDTMS groups on the surface of the membrane is $c_{HDTMS} = 3.13 \pm 0.04$ groups/nm^2.

Due to steric reasons, a condensation reaction of one HDTMS molecule with only one hydroxyl group can be assumed [4]. Therefore, a hydroxyl concentration on the membrane surface of at least 3.13 ± 0.04 groups/nm^2 can be approximated. According to literature data, this is a reasonable value compared with 8–15 hydroxyl groups/nm^2 determined by water adsorption [25–27] on ZrO_2 and 1.2 hydroxyl groups/nm^2 for a porous YSZ membrane, determined by potentiometric titration [20].

3.3. Single gas permeation measurements

The membrane structures are evaluated according to their permselectivities α_{ij} and the Knudsenselectivities $\alpha_{Kn,ij}$ as defined in Section 2.4.4. As described in Section 2.4.3, the gas permeation data is analyzed by linear regression of the molar flow onto the pressure difference. The results show a linear dependency between molar flow and pressure difference, whereas the coefficient of determination for linear regression is $R^2 > 0.999$ for all measurements. This indicates solely Knudsen flow as transport mechanism with no viscous contribution, which would result in a quadratic dependency. Furthermore, multiple measurements with CO_2 as well as N_2 at different dead-end pressures according to the measurement protocol given in Section 2.4.3 are performed. The results obtain pressure independence, assuring Knudsen flow as the governing transport mechanism (see Fig. A1). Besides, it should be noticed that a decrease in flow is observed due to HDTMS-functionalization. This behavior is already known from literature as a result for silane functionalizations [3,2,28].

In Fig. 5 the measured permselectivities are plotted against the theoretical Knudsenselectivities. The Knudsen theory is therefore represented by the bisecting line. Accordingly, measurements with membrane structures which feature solely Knudsen diffusion should show results close to the bisecting line. The higher the deviation of the measurement results from the bisecting line, the higher the contribution of an additional transport mechanism that is not described by Knudsen theory.

The non-functionalized membranes show a good agreement with the Knudsen theory and all permselectivities are very close to the bisecting line. Hence, all investigated gases (Ar, N_2, CO_2 and CH_4) propagate through the membrane following the principle of Knudsen diffusion.

After functionalization with HDTMS, not all permselectivities are in agreement with the Knudsen theory (Fig. 5). The permselectivities regarding Ar, N_2 and CH_4 meet their theoretical expectations, showing good agreement for $\alpha_{N_2/Ar}$, α_{CH_4/N_2} and $\alpha_{CH_4/Ar}$, respectively. In contrast, the permselectivities regarding CO_2 show lower values as shown for α_{Ar/CO_2}, α_{N_2/CO_2} and α_{CH_4/CO_2}. Here, all permselectivities of gas pairs containing CO_2 deviate about 20% from the theoretical values. According to the definitions in Section 2.4.4, CO_2 serves as denominator regarding these particular selectivities, since CO_2 is the heaviest gas investigated. Therefore, these smaller permselectivities in relation to CO_2 represent an enhanced flow of CO_2 compared with Ar, N_2 and CH_4 due to HDTMS-functionalization, since all other permselectivities show a behavior according to the Knudsen theory.

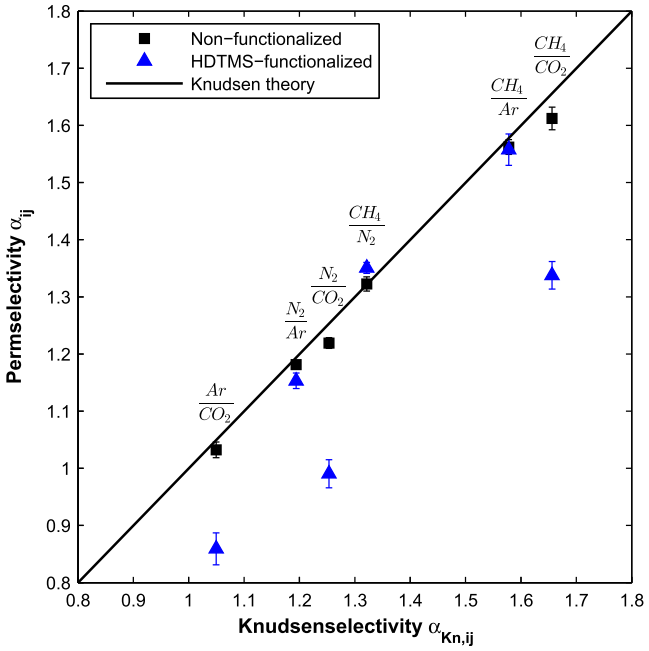

Fig. 5. Permselectivity versus Knudsenselectivity of the non-functionalized and HDTMS-functionalized membranes. The black line represents the Knudsen selectivity proposed by the Knudsen theory. The selectivities regarding CO_2 deviate from the theory after functionalization with HDTMS.

In Section 3.1 (Fig. 3 and Table 1) the membrane structures of the non-functionalized and the HDTMS functionalized membranes are discussed. The results show similar pore sizes ($d_{50,non-f.} = 22.2$ nm, $d_{50,HDTMS-f.} = 18.1$ nm), ensuring the comparability of the governing gas transport mechanism in both membrane types. Furthermore, Section 3.2 examines the presence of HDTMS molecules in the functionalized membranes, which can be estimated to 3.13 ± 0.04 functional groups/nm^2. By summarizing the microstructural and membrane surface analysis, the membrane surface chemistry is altered without changing the important membrane parameter for Knudsen flow. According to the literature, gases propagating through such mesoporous structures with pores >10 nm should follow the laws of Knudsen diffusion [16]. A potential surface diffusion is supposed to affect the gas flow significantly at smaller pores in the lower mesoporous region [12,14,15] and not at pore sizes as big as 20 nm. Nevertheless, an unexpected deviation regarding CO_2 is observed due to the surface functionalization with HDTMS. The decreasing permselecitivities for CO_2 indicate an enhanced gas flow of CO_2 compared to Ar, N_2 and CH_4. Accordingly, there is no influence of the surface functionalization on the gas flow of Ar, N_2 and CH_4. Both, the non-functionalized and the HDTMS-functionalized membrane structures are considered comparable, because the pore size distributions remain similar. Thus, the decrease in selectivity regarding CO_2 represents a specific influence of the surface chemistry on the gas flow of CO_2. This indicates that Knudsen diffusion may be the governing transport mechanism in both membrane types, but for an HDTMS-functionalized membrane it seems not to be the only one. A changed adsorption behavior of the CO_2 molecules with the surface functional groups is proposed as the influencing factor. It is hypothesized that the change in adsorption dynamics due to HDTMS-functionalization affects the gas flow of CO_2. These assumptions are further discussed based on gas adsorption/desorption measurements.

3.4. Gas adsorption and desorption measurements

An alternation of the surface functional group composition due to the functionalization with HDTMS changed the flow behavior of CO_2 in comparison to Ar, N_2 and CH_4 (Fig. 5). To further investigate the impact of HDTMS functionalization on the interaction between gas molecules and membrane surface, adsorption/desorption measurements are performed. The thermal conditions are kept similar to the gas permeation measurements (20 °C) using CO_2 and N_2 as test gases. Fig. 6 shows the adsorbed amount of molecules, given in μmol/m^2, in relation to the equilibrium pressure (in *kPa*). For both membrane types, a higher adsorption capacity is observed for CO_2 in contrast to N_2. This result is reasonable, since N_2 is an inert gas. Nevertheless, both applied test gases show significantly lower values for the HDTMS-functionalized membranes than for the untreated material. Stoltenberg and Seidel-Morgenstern [2] also detected a decrease in the adsorbed amount of CO_2 per unit volume after an amine functionalization of a mesoporous glass membrane (mean pore diameter of 3.3 nm). The decrease in specific surface area after functionalization is suggested as reason for the decreased amount of adsorbed CO_2. In the present study, the exact amount of surface area of the measured membrane pieces is determined by BET method and used as a reference value. Therefore, the decrease of the specific surface area due to the applied HDTMS-functionalization can be excluded as reason for the decreased amount of adsorbed CO_2. In summary, considering a finite surface area fraction, less molecules will adsorb on a surface with HDTMS-functionalization than without functionalization. Besides the decrease of the total amount of adsorbed molecules, the adsorption selectivity of CO_2/N_2 is significantly increased. Comparing the maximum amount of adsorbed molecules for CO_2 and N_2, given in Fig. 6, the ratio of CO_2-molecules/N_2-molecules is around four times higher for the HDTMS-functionalized membrane.

The measured decrease of adsorption capacity is assumed to be caused by a weaker interaction between gas molecules and surface due to the functionalization with HDTMS. This can be supported by quantum calculations conducted by Yu et al. [29], which show a smaller binding energy of CO_2 with alkyl-chains in comparison to functional groups with a higher polarity and therefore a smaller adsorption enthalpy at a given pressure and temperature.

Analyzing the results from both measurement techniques, an influence from the HDTMS-functionalization on gas permeation as well as gas adsorption/desorption behavior is observed. The HDTMS-functionalized membranes show a CO_2 flow which is enhanced disproportionately with respect to Ar, N_2 and CH_4 (Fig. 5). This leads to smaller permselectivities deviating from Knudsen theory. Furthermore, these membranes show a lower specific adsorption capacity for CO_2 and N_2 (Fig. 6). These altered interactions between gas molecules and surface due to the HDTMS-functionalization are claimed as reason for the change in permselectivity in contrast to the Knudsen theory. One possible explanation for the measured decrease of adsorption capacity is a weaker interaction and a smaller binding energy of CO_2 with the alkyl-functionalized surface [29] and therefore a smaller adsorption enthalpy at a given pressure and temperature. According to the literature, the amount of available adsorption sites, as well as the adsorption enthalpy have a great influence on the mechanism of surface diffusion [2,30–32]. In fact, there is an interplay between adsorption sites, adsorption strength and the amount of molecules which are adsorbed on a surface under certain conditions of pressure and temperature. Under the applied conditions of 20 °C and 800 mbar, a surface functionalization with HDTMS results in a decrease of the adsorbed amount of molecules on the surface, while increasing the selective adsorption of CO_2/N_2, along with a measurable influence on the gas permeation for CO_2. According to the general opinion from the literature adsorption effects and surface diffusion are negligible in pores >10 nm. In this case, surface diffusion may be a possible explanation for the observed deviations in gas permeation, assuming that the altered surface chemistry results in more favorable adsorption conditions for surface diffusion. A definite statement or a prove for surface diffusion cannot be given at this point, therefore this remains as an assumption. Further research is needed to fully understand the gas–solid interactions and diffusion mechanisms at these length scales.

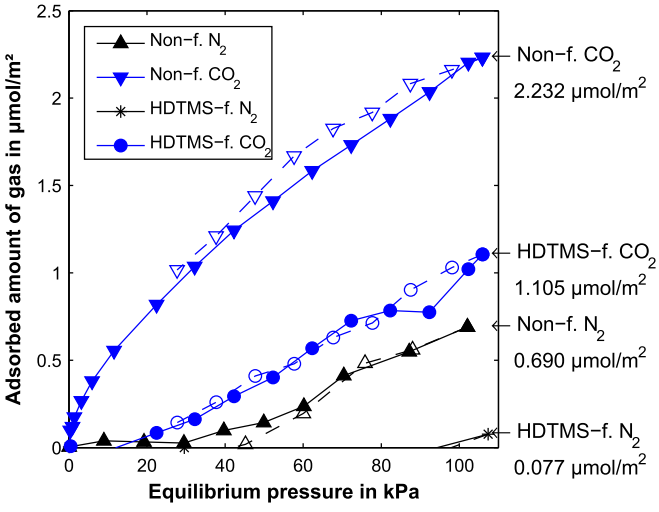

Fig. 6. N_2 and CO_2 adsorption–desorption isotherms at 20 °C for non-functionalized and HDTMS-functionalized membranes. Filled symbols are used for adsorption, empty symbols for desorption. The measured adsorbed amount is normalized to the specific surface area of the particular membrane samples and given in μmol/m^2. The adsorption capacity is decreased due to the surface functionalization.

4. Conclusion

Mesoporous YSZ capillary membranes with mean pore diameters of around 20 nm are prepared to investigate the influence of a surface functionalization with HDTMS on gaseous flows in mesoporous structures. Before and after functionalization, the membranes feature a similar pore structure with comparable mean pore diameters. Therefore, the crucial membrane property for quantification of gaseous rarefaction, the mean pore diameter, is not affected, ensuring equal flow conditions in both membrane types. Single gas permeation measurements at 20 °C are performed to investigate the influence of the altered surface characteristics on four different gases (Ar, N_2, CO_2 and CH_4). Whereas the non-functionalized membranes show ideal Knudsen diffusion behavior, the HDTMS-functionalized membranes show permselectivities differing about 20% from the Knudsen theory regarding CO_2. This reveals an enhanced CO_2 flow compared to the other gases due to HDTMS-functionalization. Adsorption/desorption isotherms also measured at 20 °C show a significant reduction of the specific adsorption capacity for CO_2 as well as N_2 after functionalization with HDTMS, suggesting a weaker interaction of the gases with the membrane surface. Furthermore, the adsorption selecitvity of CO_2/N_2 is increased. The detected adsorption effects are proposed as a reason for the deviation of the gas flow from the Knudsen diffusion theory. According to the literature, Knudsen diffusion is supposed to be the driving mechanism for gas flows at the present length scale and that adsorption effects along with surface diffusion are negligible. In contrast, the presented results

lead to the conclusion that adsorption effects also play a role in pores of the upper mesoporous region (10–50 nm) and that the contribution of molecule–surface interactions to gas transport in mesoporous structures is not fully understood yet. Surface diffusion may be a possible explanation for the aforementioned deviation from Knudsen theory. Even though, further research is needed to clearly identify all mechanisms affecting the gas flow behavior in this pore size range.

Acknowledgments

This work was supported by German Research Foundation (DFG) within the Research Training Group GRK 1860 "Micro-, meso- and macroporous nonmetallic Materials: Fundamentals and Applications" (MIMENIMA). The support of Petra Witte (University of Bremen, Department of Geosciences) for her work with the SEM is gratefully acknowledged. Furthermore, we thank T. C. Schumacher from the University of Bremen for all the fruitful discussions and the critical feedback which helped to improve this work.

Appendix A. Supplementary data

Supplementary data related to this article can be found at http://dx.doi.org/10.1016/j.micromeso.2015.06.042.

References

[1] Y. Sakamoto, K. Nagata, K. Yogo, K. Yamada, Microporous Mesoporous Mater. 101 (1–2) (2007) 303–311, http://dx.doi.org/10.1016/j.micromeso.2006.11.007. URL, http://dx.doi.org/10.1016/j.micromeso.2006.11.007.

[2] D. Stoltenberg, A. Seidel-Morgenstern, Microporous Mesoporous Mater. 154 (2012) 148–152, http://dx.doi.org/10.1016/j.micromeso.2011.11.013. URL, http://dx.doi.org/10.1016/j.micromeso.2011.11.013.

[3] S. Higgins, W. DeSisto, D. Ruthven, Microporous Mesoporous Mater. 117 (1–2) (2009) 268–277, http://dx.doi.org/10.1016/j.micromeso.2008.06.030. URL, http://dx.doi.org/10.1016/j.micromeso.2008.06.030.

[4] L. Treccani, T. Yvonne Klein, F. Meder, K. Pardun, K. Rezwan, Acta Biomater. 9 (7) (2013) 7115–7150, http://dx.doi.org/10.1016/j.actbio.2013.03.036. URL, http://dx.doi.org/10.1016/j.actbio.2013.03.036.

[5] K.L. Mittal, Silanes and Other Coupling Agents, Vol. 5, Koninklijke Brill NV, Leiden, The Netherlands, 2009.

[6] G.T. Hermanson, in: G.T. Hermanson (Ed.), Bioconjugate Techniques, Third ed., Academic Press, Boston, 2013, pp. 535–548. URL, http://www.sciencedirect.com/science/article/pii/B9780123822390000133.

[7] C. Chen, J. Kim, W.-S. Ahn, Korean J. Chem. Eng. 31 (11) (2014) 1919–1934, http://dx.doi.org/10.1007/s11814-014-0257-2. URL, http://dx.doi.org/10.1007/s11814-014-0257-2.

[8] T.-L. Chew, A.L. Ahmad, S. Bhatia, Adv. Colloid Interface Sci. 153 (1–2) (2010) 43–57, http://dx.doi.org/10.1016/j.cis.2009.12.001. URL, http://dx.doi.org/10.1016/j.cis.2009.12.001.

[9] M. Ostwal, R.P. Singh, S.F. Dec, M.T. Lusk, J.D. Way, J. Membr. Sci. 369 (2011) 139–147, http://dx.doi.org/10.1016/j.memsci.2010.11.053.

[10] R.P. Singh, J.D. Way, S.F. Dec, J. Membr. Sci. 259 (1–2) (2005) 34–46, http://dx.doi.org/10.1016/j.memsci.2005.03.004. URL, http://www.sciencedirect.com/science/article/pii/S0376738805001973.

[11] K. Kuraoka, Y. Chujo, T. Yazawa, J. Membr. Sci. 182 (1–2) (2001) 139–149, http://dx.doi.org/10.1016/S0376-7388(00)00559-7. URL, http://www.sciencedirect.com/science/article/pii/S0376738800005597.

[12] A. Lindbråthen, M.-B. Hägg, J. Membr. Sci. 259 (1–2) (2005) 145–153. URL, http://dx.doi.org/10.1016/j.memsci.2005.03.056, http://www.sciencedirect.com/science/article/pii/S0376738805003078.

[13] W.J. Koros, R. Mahajan, J. Membr. Sci. 175 (2) (2000) 181–196, http://dx.doi.org/10.1016/S0376-7388(00)00418-X. URL, http://www.sciencedirect.com/science/article/pii/S037673880000418X.

[14] R. Krishna, J. van Baten, Chem. Eng. Sci. 64 (5) (2009) 870–882, http://dx.doi.org/10.1016/j.ces.2008.10.045. URL, http://dx.doi.org/10.1016/j.ces.2008.10.045.

[15] D.M. Ruthven, W. DeSisto, S. Higgins, Chem. Eng. Sci. 64 (13) (2009) 3201–3203, http://dx.doi.org/10.1016/j.ces.2009.03.049. URL, http://dx.doi.org/10.1016/j.ces.2009.03.049.

[16] A.D. Wiheeb, M.A. Ahmad, M.N. Murat, J. Kim, M.R. Othman, Transp. Porous Media 104 (1) (2014) 133–144, http://dx.doi.org/10.1007/s11242-014-0324-5. URL, http://dx.doi.org/10.1007/s11242-014-0324-5.

[17] J. Werner, B. Besser, C. Brandes, S. Kroll, K. Rezwan, J. Water Process Eng. 4 (2014) 201–211, http://dx.doi.org/10.1016/j.jwpe.2014.10.007. URL, http://dx.doi.org/10.1016/j.jwpe.2014.10.007.

[18] S. Kroll, M.O.C. de Moura, F. Meder, G. Grathwohl, K. Rezwan, J. Eur. Ceram. Soc. 32 (16) (2012) 4111–4120, http://dx.doi.org/10.1016/j.jeurceramsoc.2012.07.026. URL, http://www.sciencedirect.com/science/article/pii/S0955221912004220.

[19] S. Kroll, L. Treccani, K. Rezwan, G. Grathwohl, J. Membr. Sci. 365 (1–2) (2010) 447–455. URL, http://www.sciencedirect.com/science/article/pii/S0376738810007568.

[20] S. Kroll, C. Brandes, J. Wehling, L. Treccani, G. Grathwohl, K. Rezwan, Environ. Sci. Technol. 46 (16) (2012) 8739–8747, http://dx.doi.org/10.1021/es3006496. URL, http://dx.doi.org/10.1021/es3006496.

[21] S. Kroll, C. Soltmann, D. Koch, P. Kegler, A. Kunzmann, K. Rezwan, Ceram. Int. 40 (10) (2014) 15763–15773, http://dx.doi.org/10.1016/j.ceramint.2014.07.100. URL, http://dx.doi.org/10.1016/j.ceramint.2014.07.100.

[22] T. Veltzke, M. Baune, J. Thöming, Phys. Fluids (1994-present) 24 (8) (2012), http://dx.doi.org/10.1063/1.4745004. URL, http://dx.doi.org/10.1063/1.4745004.

[23] T. Veltzke, On Gaseous Microflows under Isothermal Conditions, Dissertation, University of Bremen, 2013. URL, http://nbn-resolving.de/urn:nbn:de:gbv:46-00103106-14.

[24] M. Knudsen, The Law of the Molecular Flow and Viscosity of Gases Moving through Tubes, 28, Annalen der Physik, Leipzig, 1909, pp. 75–130.

[25] J. Randon, A. Larbot, A. Julbe, C. Guizard, L. Cot, Key Eng. Mater. 61–62 (1992) 495–498, http://dx.doi.org/10.4028/www.scientific.net/kem.61-62.495. URL, http://dx.doi.org/10.4028/www.scientific.net/KEM.61-62.495.

[26] J. Nawrocki, M. Rigney, A. McCormick, P. Carr, J. Chromatogr. A 657 (2) (1993) 229–282. URL, http://www.sciencedirect.com/science/article/pii/002196739380284F.

[27] J. Nawrocki, P. Carr, M.J. Annen, S. Froeliche, Anal. Chim. ACTA 327 (3) (1996) 261–266, http://dx.doi.org/10.1016/0003-2670(96)00110-9.

[28] A. Marković, D. Stoltenberg, D. Enke, E.-U. Schlünder, A. Seidel-Morgenstern, J. Membr. Sci. 336 (1–2) (2009) 17–31. URL, http://dx.doi.org/10.1016/j.memsci.2009.02.031, http://www.sciencedirect.com/science/article/pii/S0376738809001677.

[29] D. Yu, S. Matteucci, E. Stangland, E. Calverley, H. Wegener, D. Anaya, J. Membr. Sci. 441 (2013) 137–147, http://dx.doi.org/10.1016/j.memsci.2013.03.052. URL, http://dx.doi.org/10.1016/j.memsci.2013.03.052.

[30] A. Marković, D. Stoltenberg, D. Enke, E.-U. Schlünder, A. Seidel-Morgenstern, J. Membr. Sci. 336 (1–2) (2009) 32–41. URL, http://dx.doi.org/10.1016/j.memsci.2009.02.030, http://www.sciencedirect.com/science/article/pii/S0376738809001689.

[31] A. Lindbråthen, M.-B. Hägg, J. Membr. Sci. 259 (1–2) (2005) 154–160. URL, http://www.sciencedirect.com/science/article/pii/S037673880500308X.

[32] E.R. Gilliland, R.F. Baddour, G.P. Perkinson, K.J. Sladek, Ind. Eng. Chem. Fund. 13 (2) (1974) 95–100, http://dx.doi.org/10.1021/i160050a001. URL, http://dx.doi.org/10.1021/i160050a001.